Spectrum Sensing Methods and Their Performance

Chintha Tellambura

Contents

C. Tellambura (✉)
Electrical and Computer Engineering, University of Alberta, Edmonton, AB, Canada
e-mail: ct4@ualberta.ca

© Springer Nature Singapore Pte Ltd. 2017

W. Zhang (ed.), *Handbook of Cognitive Radio*,
https://doi.org/10.1007/978-981-10-1389-8_6-1

Abstract

Spectrum sensing is the process of determining if a spectrum slot is occupied or not by a primary signal. This tutorial emphasizes energy detection based spectrum sensing and provides a broad overview of the tools necessary for performance analysis of several spectrum sensing algorithms. A detailed description of the spectrum sensing problem is provided as a binary hypothesis test. The main parameters of interest – decision statistic, detection, and false-alarm probabilities and the decision threshold – are discussed. These parameters of the energy detector, which computes the energy of the received signal, are described. The use of the central limit theorem (CLT) to achieve energy detection with prescribed performance level is discussed. The receiver operating characteristic (ROC) curve and area under the curve (AUC) are described. Fading, a fundamental wireless channel impairment, can be mitigated with multiple antenna techniques, which provide spatial diversity gains. The performance of the energy detector with two low-complexity diversity techniques is described. The performance is analyzed for Rayleigh fading, for spatial correlation, and in the high signal-to-noise ratio (SNR) regime. General analytical techniques are highlighted. Double-threshold energy detector, P-norm detector, and energy detection for full-duplex nodes are described. Alternative to energy detection includes cyclostationary detection, matched filter-based detection, and waveform-based detection. These methods are briefly discussed. Spectrum sensing is an essential part of smart grid, Internet of things, and cognitive radio. An overview is provided.

Introduction

The growth of global mobile wireless networks is exponential and robust. It is driven by the use of smartphones, tablets, laptops, and other wireless devices that allow subscribers to browse the Web, use email, and download videos, multimedia, and applications. For example, by 2021, the monthly mobile data traffic will exceed 49 exabytes, mobile devices per capita will be 1.5, the wireless connection rate will increase to 20 Mbps, over 50% of mobile connections will be from smartphones, and mobile-to-mobile connections will be the majority [1].

Consequently, increasing demands for wireless mobile broadband are likely to outstrip the available radio spectrum. For example, while the 0.1–5 GHz band is perhaps the most advantageous for communications, much of it has already been allocated to about 40 different radio services such as fixed, mobile, satellite, amateur, radio navigation and radio astronomy. In fact, International Telecommunication Union (ITU) divides spectrum in to bands and assigns them to these services in order to avoid radio interference [30]. Moreover, although frequencies above 5 GHz offer the potential vast bandwidths, high attenuation, blockage, and other impairments pose significant difficulties. Therefore, spectrum congestion may hem the rapid growth of next-generation (e.g., 5G) wireless networks and users.

One potential solution is to note that much of the current licensed/assigned spectrum remains unused at different times and/or locations. Those temporary

spectrum slots (aka spectrum holes or white spaces) [19, 39] can be as high as 15–85% of the licensed spectrum [29]. Radio nodes that can identify and utilize such spectrum holes while minimizing potential interference on licensed users (aka primary users) are called cognitive radios (aka secondary users). They clearly improve overall spectrum usage, alleviating the need for new spectrum. The process of identification of spectrum holes is called spectrum sensing.

Depending on when a secondary user accesses a primary spectrum slot regardless if it is occupied or not, there are three different cognitive radio paradigms [30]:

1. Interweave – secondary user transmits only in an unused spectrum hole currently unoccupied by a primary user. To do so, secondary user must know if primary signals are present or absent in the frequency band. Thus, this paradigm clearly needs spectrum sensing.
2. Underlay – secondary user is allowed to transmit in both unused and used spectrum slots. In the latter, secondary user must adjust its transmission power such that interference on primary network is below a certain threshold. Again, the secondary requires spectrum sensing, for instance, to determine its transmit power levels.
3. Overlay – the secondary access mechanism is similar to that of underlay mode. However, secondary user earns the right to spectrum access by helping to enhance primary communication capability and by taking suitable measures to limit interference on the primary network. To achieve these two goals, secondary user needs to know some characteristics of primary signals (e.g., modulation formats, frequency, and more) in advance. This information is then used to improve communication quality of both the primary and secondary users. For example, secondary user may take proactive signal coding solutions to cancel interference on primary network. To enhance primary rates, secondary user can relay primary data. Thus, in this paradigm, secondary user must acquire much more primary information than is the case with overlay and underlay modes. Nevertheless, a critical part of the overall acquisition process is spectrum sensing.

Overall, since spectrum is essential to all the three paradigms, solid understanding of the performance of sensing algorithms in different propagation environments and in network configurations is necessary. The reliability and performance can be quantified with rigorous analytical techniques. Before discussing the basics of the performance analysis, it should be mentioned that standards with spectrum sensing include IEEE 802.22 WRAN (wireless regional area network) and its amendments, IEEE 802.11af for wireless LANs, IEEE 1900.x series, and licensed shared access (LSA) for LTE mobile operators [17]. In particular, WRAN is cognitive radio designed to operate in empty TV bands, which provides additional spectrum for wireless mobile networks on a non-interfering basis.

This tutorial aims to provide a broad overview of the tools necessary for performance analysis of spectrum sensing algorithms, with particular emphasis on energy detection. The tutorial is organized as follows:

1. The spectrum sensing problem is formulated as a binary hypothesis test. The decision statistic, detection, false-alarm probabilities, and decision threshold are discussed. The energy detector, one of the most common sensing algorithms, is described in terms of its basic performance parameters. The use of CLT to estimate the number of samples needed for the energy detection with prescribed performance level is discussed. The ROC curve and AUC are described.
2. Fading is mitigated by the use of multiple antenna techniques, which provide spatial diversity gains. The performance of the energy detector with selection and combining diversity techniques is described. Moreover, the performance is analyzed for Rayleigh fading, for spatial correlation, and in the high-SNR regime. General analytical techniques based on probability density function (PDF) and moment generating function (MGF) are highlighted.
3. Double-threshold energy detector, P-norm detector, and energy detection for full-duplex nodes are described. Alternative to energy detection includes cyclostationary detection, matched filter-based detection, and waveform-based detection. These methods are briefly discussed.
4. An overview of spectrum sensing for smart grid, Internet of things, and cognitive radio is provided.

Spectrum Sensing Problem Formulation

Clearly, accurate, reliable, and low-complexity spectrum sensing is essential for opportunistic spectrum access. To this end, secondary nodes must detect the presence/absence of a primary signal in a given frequency band $[f_0, f_1]$ for a particular time slot. This process is commonly called spectrum sensing. It can be readily formulated as a binary hypothesis test. For example, the complex signal observed at time t by the secondary user in the desired band $[f_0, f_1]$ may be modeled as [47]

$$y(t) = \begin{cases} n(t) & : H_0 \\ h(t)s(t) + n(t) & : H_1 \end{cases} \tag{1}$$

where $n(t)$ is an additive complex white Gaussian noise process, $h(t)$ represents a fading process (e.g., nonfading means $h(t) = 1$), and $s(t)$ is a signal transmitted by the primary node [47]. The sensing decisions are made using $N \gg 1$ samples of $y(t)$. The choice of N will be discussed later. Starting with this observational model, it is possible to formulate a wide array of spectrum sensing techniques based on signal energy, matched filtering, cyclostationary features, covariances, and others. These will be discussed subsequently.

Let $y(k)$ be the k-th ($k = 1, 2, \ldots, N$) sample of $y(t)$. All the samples are placed in to the vector $\mathbf{y} = [y(1), \ldots, y(n)]'$. These samples are used to compute a decision statistic $T(\mathbf{y})$. The hypothesis test for spectrum sensing is then given by

$$\text{if} \begin{cases} T(\mathbf{y}) < \lambda & \text{accept} \quad : H_0 \\ T(\mathbf{y}) > \lambda & \text{accept} \quad : H_1 \end{cases} \tag{2}$$

where $0 < \lambda < \infty$ is called the decision threshold. The reliability associated with the decision the rule (2) can be characterized by probability of detection P_d and probability of false alarm P_f. The former is the probability of detecting the primary signal when it is actually present in the frequency band, $[f_0, f_1]$. Consequently, large detection probability is highly desirable. Mathematically, it is a conditional probability given by

$$P_d = \Pr(T(\mathbf{y}) > \lambda | H_1).$$

Equivalently, the complement of this probability $P_{md} = 1 - P_d$ is also widely used for illustration and design purposes.

On the other hand, the test might incorrectly decide that $s(t)$ is present in $[f_0, f_1]$ when it actually is not, and this false-alarm probability may be written as

$$P_f = \Pr\left(T(\mathbf{y}) > \lambda | H_0\right).$$

The exact values of P_d and P_f depend on how $T(\mathbf{y})$ is constructed using received samples, channel estimates, propagation characteristics, the choice of the threshold, and other information. The false alarms will clearly reduce spectrum access opportunities for secondary users, and hence the expected improvements in spectral efficiency are not materialized. This problem may be alleviated by choosing the decision threshold λ for an optimum balance between P_d and P_f. However, this requires knowledge of noise and detected signal powers. Estimation of both noise power and signal power can be challenging as they are depend on evolving transmission standards and the locations of primary and secondary nodes. In practice, with the knowledge of noise variance, the threshold is chosen to obtain a certain false-alarm rate (section "Threshold Optimization Techniques").

Notations

$\mathbb{P}(\cdot)$, $\mathbb{E}(\cdot)$, $\mathrm{Var}(\cdot)$ denote the probability measure, expectation, and variance. $\Gamma(z) = \int_0^\infty t^{z-1}e^{-t}dt$, $\Gamma(z,x) = \int_x^\infty t^{z-1}e^{-t}dt$, ${}_2F_1(a,b;c;z) = \sum_{k=0}^\infty \frac{(a)_k(b)_k(z)^k}{(c)_k k!}$ is the Gauss hypergeometric function, with $(x)_y$ denoting the Pochhammer symbol. If $X_1, \ldots, X_k$ are independent Gaussian $N(0, \mu_k)$ random variables, then $Y = \sum_{i=1}^k X_i^2$, is noncentral chi-square, $\chi_k^2(\delta)$, with k degrees of freedom and $\delta = \sum \mu_k^2$. If all $\mu_k = 0$, Y is central chi-square, χ_k^2. The generalized Marcum-Q function is $Q_l(a,b) = \int_b^\infty \frac{x^l}{a^{l-1}} e^{-(x^2+a^2)/2} I_{l-1}(ax)dx$, where $I_l(x)$ is the l-th order modified Bessel function. The Gaussian-Q function is $Q(x) = \int_x^\infty \frac{e^{-t^2/2}}{\sqrt{2\pi}}dt$.

Classical Energy Detector

As mentioned before, although the exponential growth of mobile data traffic is likely to outstrip the available spectrum, licensed users may not be active at a given spectrum slot (e.g., 54–806 MHz TV band), a time, and a location. To access those spectral holes, secondary user may first sense them via the most popular spectrum sensing algorithm: energy detector, which has thus attracted massive wireless research interest due to its simple structure and low hardware complexity [7].

This detector computes a proxy for the energy of received signal over the spectrum slot that is being tested. The basic concept is that the computed energy must be sufficiently high if the slot contains primary signals; otherwise, the slot contains noise only. Thus, this detection problem can be formulated as a special case of the hypothesis test (2) with the decision statistic given by

$$T(\mathbf{y}) = \sum_{i=1}^{N} |y_i|^2 \tag{3}$$

where y_i is the i-th ($i = 1, 2, \ldots, N$) sample of $y(t)$ and N is the number of samples. It can be readily shown that $T(\mathbf{y})$ conditional on H_0 and H_1 are distributed as central chi-square χ^2_{2N} and noncentral chi-square $\chi^2_{2N}(2\gamma)$, respectively, both with $2N$ degrees of freedom. The noncentrality parameter is 2γ where γ is the SNR. For a static channel scenario, false-alarm and detection probabilities may be expressed as

$$P_f = \Gamma(N, \lambda/2)/\Gamma(N) \tag{4}$$

$$P_d = Q_N(\sqrt{2\gamma}, \sqrt{\lambda}), \tag{5}$$

where $\Gamma(a, b)$ and $Q_N(a, b)$ are incomplete Gamma function and the Marcum-Q function, respectively. The choice of a suitable value for N has critical ramifications on both performance and complexity. The method of choosing N will be discussed in Sect. "Use of the CLT." The SNR γ is a fixed quantity if the channel is static (e.g., $h(t) = 1$); otherwise, it will be modeled as a random variable (this case will be treated subsequently).

The Eqs. (4) and (5) connect false-alarm and missed-detection probabilities with the SNR, the decision threshold, and the number of samples. Thus, many design choices and requirements can be made depending on specific requirements. For example, very low SNR is −20 dB with a signal power of −116 dBm and a noise floor of −96 dBm [7]. For this reason, IEEE 802.22 prescribes both P_d and P_f be less than 0.1. While energy detection performs well at moderate and high SNRs, low-SNR operation typically requires large N, which impacts the sensing and processing time. For example, IEEE 802.22 limits the maximal detection latency to 2 s which may include sensing time and subsequent processing time. This maximal time limit is critical at low-SNR spectrum sensing.

In the literature, the detection probability P_d has also been analyzed extensively, treating propagation characteristics, multiple antennas, cooperative diversity, and other factors [3, 5, 16, 20, 42]. However, exact analysis tends to be complicated (special functions, infinite series, and so on). Moreover, since closed-form P_d for more complicated versions of energy detection appears intractable, several computational methods have been developed [40]. To detect potential spectrum opportunities rapidly, sensing algorithms must operate with the fewest possible number of samples and offer high reliability. Therefore, selection of a suitable number of samples, N, is considered next.

Use of the CLT

When the number of samples N is sufficiently large, CLT can be used instead of the exact equations (4) and (5) [7]. Thus, false-alarm and detection probabilities may be approximated as

$$P_{f,CLT} \approx Q\left(\frac{\lambda - 2N}{2\sqrt{N}}\right) \tag{6}$$

$$P_{d,CLT} \approx Q\left(\frac{\lambda - 2N(1+\gamma)}{2(1+\gamma)\sqrt{N}}\right) \tag{7}$$

where primary signal $s(t)$ is assumed to be zero-mean, complex Gaussian and $Q(x)$ is the standard Gaussian upper tail probability function. Although it is possible to consider different models for $s(t)$, the details are omitted for brevity. This approximation has been utilized to investigate sensing-throughput tradeoff [28], multiple-band spectrum sensing [35], low-SNR spectrum sensing [6, 31], and numerous others. However, it may not be accurate enough for small sample sizes [37].

Next the above is used to determine the suitable sample size N. Suppose the prescribed performance point is (P_f, Pd). By using (6) and (7), and solving for N, it turns out that

$$N \approx \left[\gamma^{-1}Q^{-1}(P_f) - (1+\gamma^{-1})Q^{-1}(P_d)\right]^2.$$

Based on the CLT, this estimate may be accurate only when N is sufficiently high but not when P_f is low and P_d is high [37]. To get around these challenges, [37] has developed an estimate of N using the cube-of-Gaussian approximation (CGA), and further results have been reported in [9, 38].

Threshold Optimization Techniques

In (2), the key parameter is the decision threshold, λ. This threshold must be optimized for each detection technique to improve its performance. The threshold

may be chosen by considering P_f and P_d. A common practice is to set the threshold is based on a constant false-alarm probability, say, P_f. For example, then based on the normalized threshold is

$$\lambda^* = 2\sqrt{N}\left(Q^{-1}(P_f) + \sqrt{N}\right)$$

which must adjusted based on the variance of the additive noise. Note that P_d and P_f are functions of λ. In general, it is chosen to make P_d large and P_f small as possible (e.g., in IEEE 802.22 WRAN needs $P_f \leq 0.1$ and $P_d \geq 0.9$). More generally, the threshold may be optimized by considering noise level, total error rate, and other factors [7].

ROC Curves

Although detection (or missed detection) and false-alarm probabilities are key measures, detection capability is typically illustrated with a so-called ROC curve – a plot of the detection probability versus the false-alarm probability when the threshold varies from 0 to ∞. Thus, the ROC curve is defined parametrically as pair (x, y) with

$$x = P_f(\lambda) \quad y = P_d(\lambda), \quad 0 \leq \lambda < \infty. \tag{8}$$

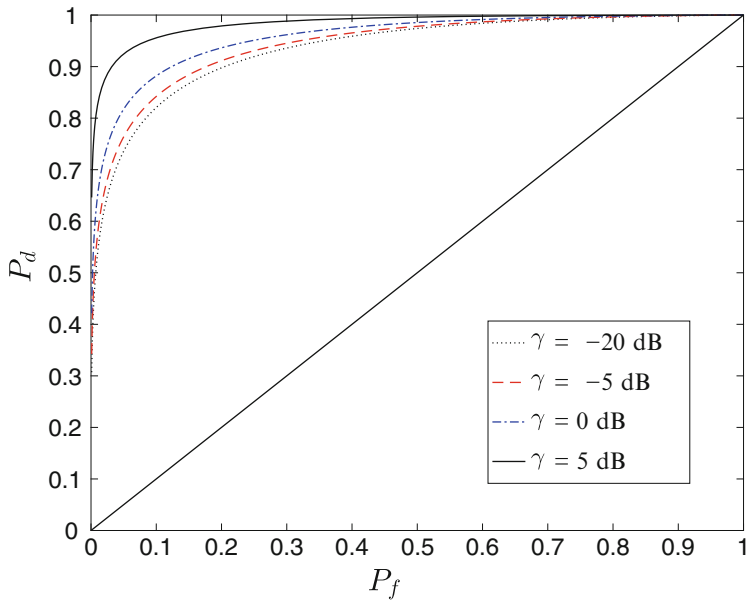

Fig. 1 ROC for energy detection

A set of ROC curves for the basic energy detector ($N = 10$) in a static channel is depicted in Fig. 1. Each ROC curve corresponds to a particular SNR, γ. The upper left corner or coordinate (0,1) of the ROC space, representing 0% false alarms and 100% detection, depicts the best possible detector. The diagonal line ($P_d = P_f$) from the left bottom to the top right corners depicts a random detector such as detection by flipping coins (heads or tails). The further away is the ROC curve from the diagonal, the better is the detector performance. The ROC figures have been widely used to illustrate the energy detector performance for small-scale and large-scale fading, diversity reception techniques, and cooperative spectrum sensing [7].

However, a single summarizer of detection capability is also desirable. This is called area under the ROC curve (AUC) [2]. The AUC is a number between 0 and 1, and a perfect detector has an AUC of 1. Moreover, an AUC of 0.5 represents a random detector (e.g., coin flip). In fact, the more far AUC is from 0.5, the better is performance. If AUC is below 0.5, the detector output must be inverted. For example, if AUC is zero, the inverted detector output yields a perfect decision. The AUC may be evaluated as

$$\mathscr{A} = \int_0^1 P_d \, dP_f. \tag{9}$$

By substituting the values of P_d and P_f from (5) and (4), the AUC of classical energy detector can be obtained as [2]

$$\mathscr{A}(\gamma) = 1 - \sum_{k=0}^{u-1} \frac{1}{2^k k!} \gamma^k e^{\frac{-\gamma}{2}} + \sum_{k=1-u}^{u-1} \frac{\Gamma(u+k)}{2^{u+k}\Gamma(u)} e^{-\gamma} \, {}_1F_1\left(u+k; 1+k; \frac{\gamma}{2}\right) \tag{10}$$

where ${}_1F_1(a, b, c)$ is the regularized confluent hypergeometric function. The expression (10) shows that as SNR tends to infinity, the AUC approaches one, which is desirable.

AUC and complementary AUC (CAUC) (e.g., $1 - \mathscr{A}$) have been derived for an energy detector with no diversity reception, with several popular diversity schemes, with channel estimation errors, with fading correlations, and with relay signaling [2] and [4]. However, the analysis of [2,4] may not work for cooperative spectrum sensing. Moreover, special functions (e.g., Marcum-Q and confluent and regularized confluent hypergeometric functions) in P_d make closed-form evaluation of the AUC rather intractable. To circumvent these drawbacks, AUC can be related to the MGF of the received SNR. The resulting calculations are simple, avoid special functions, and are readily available in modern mathematical platforms (e.g., Mathematica and MAPLE). This approach will be developed in Sect. "MGF-Based Approach."

Performance in Fading Channels

Wireless channel impairments include small-scale fading, shadowing, and path loss [18,32]. Modeling these impairments is critical to characterize and analyze spectrum

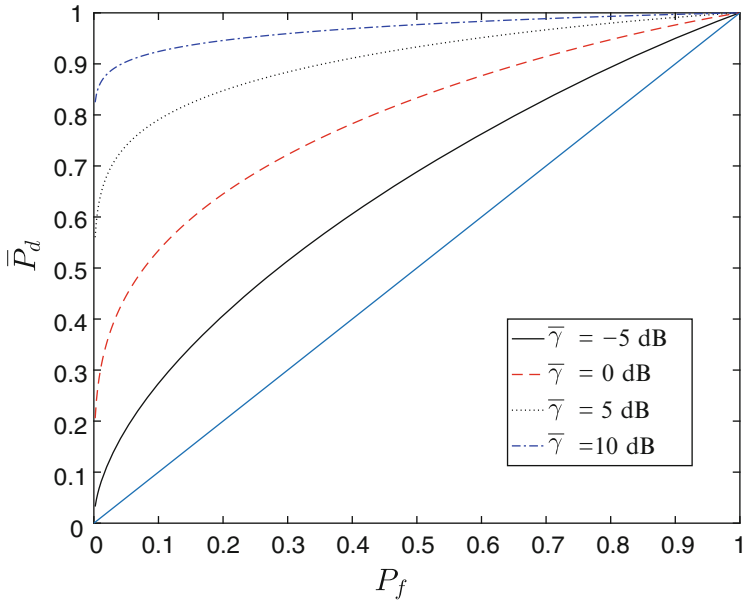

Fig. 2 ROC for energy detection in a Rayleigh channel

sensing algorithms. Small-scale fading is characterized by various models such as Rayleigh, Nakagami-*m*, and Rician [32]. A detailed sensing performance analysis for these channels is beyond the scope of this tutorial. Moreover, although fading does not impact P_f (4), P_d (5) must be averaged over the distribution. For instance, the performance under Rayleigh fading (i.e., $f_\gamma(x) = \frac{1}{\bar{\gamma}} e^{-x/\bar{\gamma}}, 0 \le x < \infty$) is given as [16,21]

$$\overline{P}_d = e^{-\frac{\lambda}{2}} \sum_{i=0}^{N-2} \frac{\left(\frac{\lambda}{2}\right)^i}{i!} + \left(\frac{1+\bar{\gamma}}{\bar{\gamma}}\right)^{N-1} \times \left[e^{-\frac{\lambda}{2(1+\bar{\gamma})}} - e^{-\frac{\lambda}{2}} \sum_{i=0}^{N-2} \frac{\left(\frac{\lambda\bar{\gamma}}{2(1+\bar{\gamma})}\right)^i}{i!} \right]. \quad (11)$$

A set of ROC curves for the basic energy detector ($N = 10$) in a Rayleigh fading channel is depicted in Fig. 2. Each ROC curve corresponds to a particular SNR, $\bar{\gamma}$. The diagonal line ($\bar{P}_d = P_f$) from the left bottom to the top right corners depicts a random detector such as detection by flipping coins (heads or tails). The further away is the ROC curve from the diagonal, the better is the detector performance. Thus, note that as $\bar{\gamma}$ increases, the ROC moves away from the diagonal and toward the (0,1) point, which is the ideal performance.

Spatial Diversity for Spectrum Sensing

Spatial diversity (e.g., multiple antennas) can be exploited to mitigate fading. In the literature, a large body of research has investigated the use of $L > 1$ antennas to enhance the performance of spectrum sensing (see [7] and references therein). With multiple antenna systems, channel states of individual antenna branches and spatial correlations must be considered. These factor will complicate the analysis and operation of common energy detector. Nevertheless, two diversity schemes are briefly described next. In square-law combiner (SLC), the individual energy measurements of different antennas are added together to form the total. The decision statistics is thus $T(\mathbf{y}) = \sum_{i=}^{L} Y_i$ where Y_i is the decision statistic for the i-th antenna branch ($i = 1, \ldots, L$). The equivalent SNR is thus given by $\gamma_{SLC} = \sum_{i=1}^{L} \gamma_i$ where γ_i is the SNR associated with the i-th antenna branch ($i = 1, \ldots, L$). The final decision is made after comparing $T(\mathbf{y})$ against the threshold. The false-alarm and the detection probabilities are thus obtained as [16]

$$P_{f,SLC} = \frac{\Gamma(LN, \frac{\lambda}{2})}{\Gamma(LN)},$$

$$P_{d,SLC} = Q_{LN}\left(\sqrt{2\gamma_{SLC}}, \sqrt{\lambda}\right).$$

In square-law selection (SLS), only the branch with the largest energy is selected. The decision statistics is thus $T(\mathbf{y}) = \max(Y_1, \ldots, Y_L)$ where Y_i is the decision statistic for the i-th antenna branch ($i = 1, \ldots, L$). Thus, false-alarm and detection probabilities can be obtained as [16]

$$P_{f,SLS} = 1 - \left[1 - \frac{\Gamma\left(N, \frac{\lambda}{2}\right)}{\Gamma\left(N\right)}\right]^{L}$$

$$P_{d,SLS} = 1 - \prod_{i=1}^{L}\left[1 - Q_N\left(\sqrt{2\gamma_i}, \sqrt{\lambda}\right)\right].$$

A set of ROC curves for the basic energy detector ($N = 10$) with SLC in Rayleigh fading is depicted in Fig. 3. Each ROC curve corresponds to a particular number of antennas, L. The diagonal line ($\bar{P}_d = P_f$) from the left bottom to the top right corners depicts a random detector such as detection by flipping coins (heads or tails). The further away is the ROC curve from the diagonal, the better is the detector performance. Thus, note that as L increases, the ROC moves away from the diagonal and toward the (0,1) point, which is the ideal performance. This suggests that the spatial diversity of SLC improves the energy detector performance.

Thus far, it has been seen that the average of P_d in fading channels requires the PDF of γ. In many wireless problems, this PDF can be a highly complex expression or even intractable.

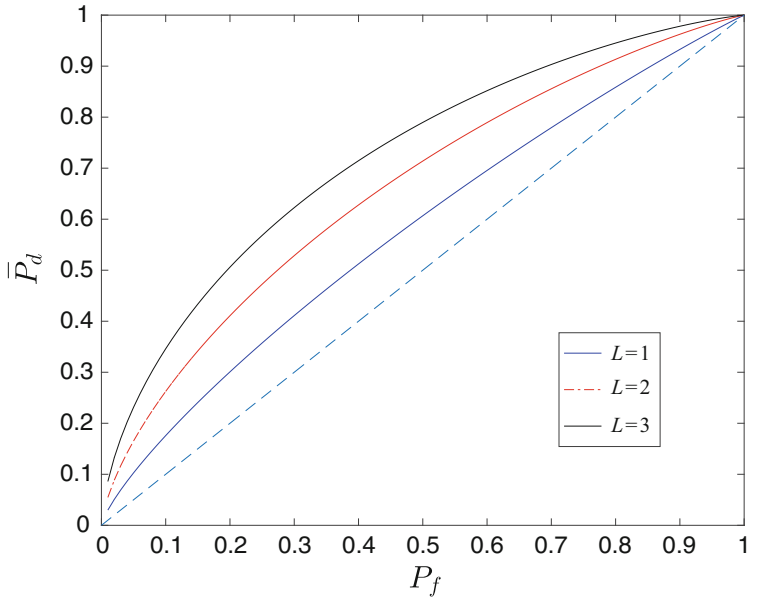

Fig. 3 ROC for energy detection and SLC for different numbers of antennas

MGF-Based Approach

To avoid such difficulties, the MGF of γ can be utilized for analysis [43–45]. The reason of this wide applicability is that MGF of a sum of independent random variables is equal to the product of individual MGFs [25, 26].

Using the alternative representation of the Marcum-Q function [44], the average of P_d (5) in a multiple antenna system can be expressed as

$$\overline{P}_d = \frac{e^{-\frac{\lambda}{2}}}{2\pi j} \oint_{\triangle} M\left(1 - \frac{1}{z}\right) \frac{e^{\frac{\lambda}{2} z}}{z^q (1-z)} dz \tag{12}$$

where MGF $M(s) = \mathbb{E}(e^{-s\gamma})$, $j = \sqrt{-1}$, $\triangle$ is a circular contour of radius $0 < r < 1$ that encloses origin, and q is a positive integer which depends on N, the number of antennas and diversity combining method. For example, with SLC described earlier, $q = LN$. The integral expression (12) can thus be customized for many diversity systems where the MGF is readily available.

This equation (12) can also be used to derive average AUC under different fading channels. Since $\bar{\mathscr{A}} = \int_0^1 \bar{P}_d dP_f$, average AUC is obtained as

$$\bar{\mathscr{A}} = \frac{1}{j2\pi} \oint_{\triangle} M\left(1 - \frac{1}{z}\right) \frac{1}{z^q (1-z)(z-2)^N} dz. \tag{13}$$

Both (12) and (13) are versatile and provide a powerful basis for analysis of energy detector with various diversity schemes (see [7] for further examples).

Antenna Correlation

Standards like the Long-Term Evolution (LTE) Advanced, WiMax, and International Mobile Telecommunications (IMT) Advanced have promised high data rate services; they motivate the use of multiple antenna terminals. With such secondary nodes, the antenna correlation is an important factor that affects the overall performance of energy detection. To illustrate the impact of antenna correlation, energy detection with SLC can be analyzed. The branch SNR's γ_i $(i = 1, \ldots, L)$ are related by a correlation matrix. The PDF of SNR may be written as

$$f_{\gamma_{SLC}}(x) = \frac{1}{\bar{\gamma}} \sum_{k=1}^{L} \frac{\pi_k}{\mu_k} e^{-x/(\bar{\gamma}\mu_k)}, \quad 0 \le x < \infty \tag{14}$$

where μ_k is the k-th eigenvalue of the correlation matrix and $\pi_k = \prod_{i \neq k} \frac{\mu_k}{\mu_k - \mu_i}$. The correlation matrix is called exponential if the ij-th entry $\rho_{ij} = \rho^{|i-j|}$. However, this model is not universal. For example, the correlation depends the placement, spacing and height of antenna elements, signal incident angles, and so on. Another common model is the Toeplitz structure where $\rho_{ij} = [\rho_{|i-j|}]$ with $\rho_0 = 1$.

For illustration purposes, consider two correlated (ρ) antennas. The two eigenvalues can be shown to be

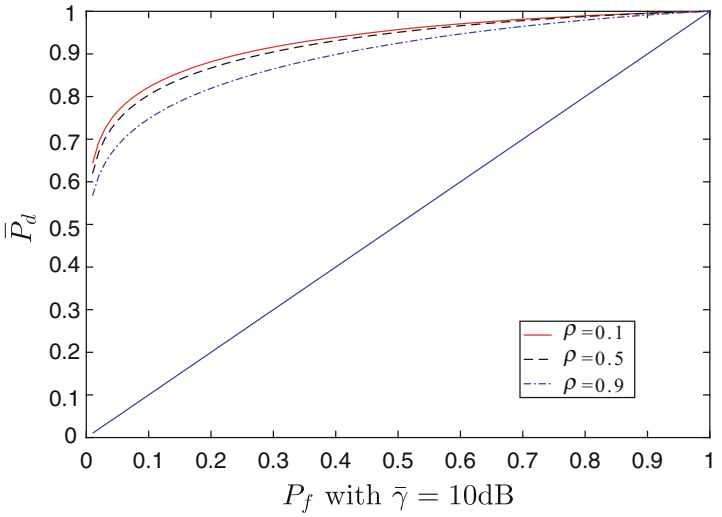

Fig. 4 ROC for SLC energy detection with antenna correlation

$$\mu_1, \mu_2 = (1 \pm \rho). \tag{15}$$

The ROC curves for this system are shown in Fig. 4. It is clear that the correlation penalizes the performance. That is, as ρ increases, the ROC curves move toward the diagonal line. The impact of correlation is not high because this is a system with two branches only. A higher impact can be expected for systems with more antennas.

Asymptotic Performance Measures

As mentioned before, the SNR γ in a fading environment is a random variable, and hence average of P_d over the distribution of γ, denoted by $\overline{P}_d$, is often computed. The details of the averaging process are as follows. First, $P_d(\gamma)$ for a fixed channel realization is given in (5). It is convenient to express SNR as the product $\gamma = \overline{\gamma}\beta$, where $\overline{\gamma}$ is the average SNR (in static channels $\beta = 1$ and $\gamma = \overline{\gamma}$), and β is a nonnegative random variable, which accounts for system conditions including channel propagation conditions, antenna diversity, interference, and others. Thus, β is characterized by PDF $f(\beta)$. In the second step, $P_d(\gamma)$ is integrated over $f(\beta)$.

The average probability detection can thus be expressed as

$$\overline{P}_d = \int_0^\infty Q_N(\sqrt{2\overline{\gamma}\beta}, \sqrt{\lambda}) f(\beta) d\beta. \tag{16}$$

Thus, the main challenge in (16) is the lack of closed-form solutions for integrals involving the Marcum-Q function or tedious analytical expressions involving complicated special functions and/or infinite series [33]. One solution is to use the MGF approach (12).

An alternative solution is to simplify $f(\beta)$ in order to facilitate the evaluation of (16) in simple yet accurate form. To this end, an idea of Wang and Giannakis [49] may be utilized. The basic concept is that in the high-SNR regime (e.g., $\bar{\gamma} \to \infty$), the integral (16) can be tightly approximated by simply using just the first term of the Taylor series expansion of $f(\beta)$ at $\beta = 0$. Thus, let exact PDF $f(\beta)$ have the monomial expansion as $\beta \to 0^+$ [49]

$$f^{\text{wg}}(\beta) = a\beta^t + O(\beta^{t+1}), \tag{17}$$

where the parameters a and t define the first term of the PDF expansion, which in turn depend on the operating conditions. These two can be obtained by utilizing the exact PDF or MGF of the diversity structure. Moreover, (17) holds for many practical fading models like Rayleigh, Nakagami-q, Nakagami-n, and Nakagami-m [49]. Further developments on (17) can be found in [14, 15].

By utilizing $f^{\text{wg}}(\beta)$, [48] has derived the asymptotic

$$\overline{P}_{md} \approx \frac{A}{\bar{\gamma}^{t+1}}, \quad \bar{\gamma} \to \infty \tag{18}$$

where A is a constant independent of $\bar{\gamma}$. This shows that for large SNRs ($\overline{\gamma} \gg 1$), missed-detection probability decreases at rate of $t + 1$ on a log-log scale. This observation leads to the notion of sensing gain, which is equal to $t + 1$. However, this approximation is accurate only in the high-SNR regime (say, $\overline{\gamma} \geq 20\,\text{dB}$). This means something other than $f^{\text{wg}}(\beta)$ is needed to approximate $\overline{P}_{md}$ which is accurate over a wider range of SNRs (say, $0 \leq \overline{\gamma} < \infty$). New approximations with such properties can be developed [14, 15, 41].

P-Norm Detection

This idea generalizes classical energy detection (19). Instead of simply squaring, the magnitudes of the signal samples are raised to power $p > 0$ [12, 31, 40]. Thus, the decision variable becomes

$$T(\mathbf{y}) = \sum_{i=1}^{N} |y_i|^p \tag{19}$$

where y_i is the i-th sample and N is the number of samples. Note that $p = 2$ reverts to the classical energy detector (Sect. "Classical Energy Detector"). Several approximations for conditional decision variables $T|H_0, T|H_1$ and probabilities P_f and P_d are analyzed in [8]. One idea is to approximate $T(\mathbf{y})$ a three-parameter gamma distribution. The approximate detection probability is given as [8]

$$P_d^{tg} = \frac{1}{\Gamma(\alpha)} \Gamma\left(\alpha, \frac{\lambda - \delta}{\beta}\right). \tag{20}$$

where δ, α, and β are calculated by cumulant matching. Using this, AUC or area under the ROC curve can be derived. This single figure of merit for P-norm detection [7] has been elusive for arbitrary sample sizes. As well, exact computational methods for P_d and P_f exploiting Talbot's method of numerical integration and Laguerre-polynomials can be found in [40].

Double Threshold Energy Detection

Although the classical energy detector has the benefits of low complexity and blind operation (e.g., without needing primary signal information), the optimum threshold value to achieve target probabilities of false alarm and detection is prone to estimation errors, e.g., noise estimation error. Moreover, these two probabilities cannot be independently adjusted to desirable levels using a single decision threshold. These

drawbacks can be alleviated with a double threshold energy detection [22], which allows independent setting of arbitrarily low P_f and P_{md} at the cost of an increased uncertainty region. For this detector, the hypothesis test is thus defined as

$$\text{if } \begin{cases} T(\mathbf{y}) < \lambda_0 & \text{accept} \ : H_0 \\ \lambda_0 \le T(\mathbf{y}) < \lambda_1 & \text{No decision} \\ T(\mathbf{y}) \ge \lambda_1 & \text{accept} \ : H_1 \end{cases} \tag{21}$$

Thus, false-alarm and detection probabilities (4) and (5) depend on λ_0 and λ_1. However, for double threshold energy detection, a new parameter of probability of uncertainty is incorporated and expressed as a function of λ_0 and λ_1. Probability of uncertainty is given by [22]

$$P_c = \frac{\Gamma(N, \lambda_0/2) - \Gamma(N, \lambda_1/2)}{\Gamma(N)} + Q_N(\sqrt{2\gamma}, \sqrt{\lambda_0}) - Q_N(\sqrt{2\gamma}, \sqrt{\lambda_1}). \tag{22}$$

If $\lambda_0 = \lambda_1$, this rule reverts to the classical (2).

Energy Detection with Full Duplex Nodes

Radio nodes typically operate in half-duplex (HD) mode, e.g., transmission and reception functions require distinct, separate time or frequency slots. However, if both functions occur simultaneously on the same frequency band, spectral efficiency potentially doubles at the cost of self-interference. Since this self-interference poses a fundamental limit, cancellation methods have been developed with recent advances in antenna design and analog/digital signal processing techniques [10]. Nevertheless, residual self-interference will limit the system performance.

This residual interference will affect the ability of a radio node to sense spectrum holes. Thus, the complex signal observed at time t by the secondary full-duplex user in the desired band $[f_0, f_1]$ may be modeled as [36]

$$y(t) = \begin{cases} d(t) + n(t) & : H_0 \\ h(t)s(t) + d(t)n(t) & : H_1 \end{cases} \tag{23}$$

where $d(t)$ is the residual self-interference signal. According to this model, the effective SNR can be expressed as [36]

$$\gamma_{FD} = \frac{\gamma_t}{\gamma_i + 1}, \tag{24}$$

where γ_t and γ_i denote SNR at transmitter and the ratio between self-interference power and thermal noise, respectively. Assuming self-interference $d(t)$ to follow

complex Gaussian with mean 0 and variance σ_i^2 [36], false-alarm and detection probabilities may be expressed as

$$P_f = \Gamma(N, \lambda/2(1+\sigma_i^2))/\Gamma(N) \tag{25}$$

$$P_d = Q_N(\sqrt{2\gamma_{FD}}, \sqrt{\lambda}/(1+\sigma_i^2)). \tag{26}$$

The ROC curves can be plotted by using these equations. Thus, it is possible to evaluate the performance of full-duplex energy detection.

Alternatives

As mentioned before, energy detection offers not only a low-complexity and low-cost solution for spectrum sensing but also avoids a prior information about primary signals. However, it sometimes performs poorly. For example, when a primary signal and multiple interfering signals are present in a band, the energy detector may not readily differentiate among these, and hence spectrum access decisions can be overly conservative. In the following, three alternatives are briefly described.

Cyclostationary Based Detection

Cyclostationarity signals are signals that exhibit periodic probability structures (e.g., periodic mean and autocorrelation). These periodicities are in turn caused by special features such as modulation formats and cyclic components of primary signals or may even be introduced deliberately in order to assist spectrum sensing. Such detection algorithms can readily differentiate H_0 from H_1 because simply additive noise does not exhibit any correlation structures. Furthermore, they may even distinguish among different types of transmissions and primary users. Their performance has been surveyed in [11, 50].

Matched Filter Based Detection

The received signal is correlated with a copy of the primary signal [7, 27]. If the primary signal and channel response are known, this detector is thus optimal (Neyman-Pearson sense) and maximizes the SNR. It can also take advantage of matched-filter implementations ion existing networks. For example, a matched filter is used by IEEE 802.11 (WiFi) nodes to detect incoming packets, and the same filter may also be leveraged to help with spectrum sensing. This detector also requires perfect timing and synchronization and thus incur computational complexity. Its performance decreases dramatically when channel response changes rapidly or when there are multiple primary user signals over the same band. However, a

matched filter can be customized for each primary signal, but the overall complexity will be high. The performance of a matched filter (noise level of one) is given in [11].

Waveform-Based Detection

Current wireless networks periodically transmit special signal patterns for synchronization or for other purposes. They include prefixes for frame delineation, pilot patterns, spreading sequences, and others [50]. Thus, such a preamble can be correlated with the received signal. Such waveform-based (WF) sensing or coherent sensing can outperform energy detector in terms of reliability and convergence time. The performance advantage increases as the length of the known signal pattern increases. WF sensing performs well even with very low SNRs.

Applications

Smart Grids

A smart electrical grid includes a variety of operational and energy measures including smart meters, smart appliances, renewable energy resources, and energy-efficient resources. The communication goals of smart grid can be served by the use of spectrum sensing. For example, [13] studied the energy detector-based spectrum sensing in smart grids and its impact on the performance of demand response management. Matched filter-based spectrum sensing may also be used. A feature detection-based spectrum sensing for smart grid has been examined in [34]. However, sophisticated spectrum sensing algorithms may require significantly high power requirements. On the other hand, cooperative energy-efficient sensing schemes are suitable for dense smart grid environments [24]. Several practical spectral sensing approaches for CR in smart grids have been surveyed in [24].

Internet of Things (IoT)

Cognitive radio is expected to have a variety of IoT applications where very large numbers of sensors will coexist in a small physical space. Thus, spectrum sensing technologies are highly important for WSAN (wireless sensor and actuator networks) based IoT and the requirements and issues related to adaptive systems and architectures [23]. WSANs generally utilize the industrial, scientific, and medical (ISM) radio bands. However, overcrowded ISM bands negatively affect WSAN performance. Thus, improved spectrum sensing and spectrum data processing must be developed [46].

Spectrum Sensing in Standards

Spectrum sensing has been considered in IEEE 802.22 (for TV white spaces) and ECMA 392 [30]. However, specific techniques are not prescribed. Thus, anyone which satisfies the false-alarm and missed-detection requirements of the standard can be chosen. Coexistence among different standards is also important. For example, in heterogeneous network settings, coexistence between IEEE 802.22 WRAN and IEEE 802.11af Super Wi-Fi in the TV white spaces may be required. However, maximum transmit power of an 802.22 node is 1 W while that for an 802.11af is 100 mW. Thus, such power disparities will affect the ability of the spectrum sensing algorithm to differentiate between presence/absence of primary signals. Moreover, its performance may also be affected by interference from random numbers of nodes located randomly.

Summary

This tutorial provides a broad overview of the tools necessary for performance analysis of spectrum sensing algorithms, with particular emphasize on energy detection. The following contributions are made.

1. The spectrum sensing problem is provided as a binary hypothesis test. The decision statistic, detection, and false-alarm probabilities and the decision threshold are discussed. The basic parameters of the energy detector are described. The use of CLT to estimate the number of samples and prescribed performance levels is discussed. The ROC and AUC are described.
2. Fading is mitigated with multiple antenna techniques, which provide spatial diversity gains. The performance is analyzed for Rayleigh fading, diversity combining, and spatial correlation and in the high-SNR regime. General analytical techniques are highlighted.
3. Double-threshold energy detector, P-norm detector, and energy detection for full-duplex nodes are described. Alternative to energy detection includes cyclostationary detection, matched filter-based detection, and waveform-based detection. These methods are briefly discussed. Spectrum sensing is an essential part of smart grid, Internet of things, and cognitive radio. An overview is provided.

References

1. Cisco visual networking index (2017) Global mobile data traffic forecast update, 2016–2021. http://www.cisco.com/c/en/us/solutions/collateral/service-provider/visual-networking-index-vni/mobile-white-paper-c11-520862.pdf
2. Atapattu S, Tellambura C, Jiang H (2010) Analysis of area under the ROC curve of energy detection. IEEE Trans Wirel Commun 9(3):1216–1225

3. Atapattu S, Tellambura C, Jiang H (2010) Performance of an energy detector over channels with both multipath fading and shadowing. IEEE Trans Wirel Commun 9(12):3662–3670
4. Atapattu S, Tellambura C, Jiang H (2010) Performance of energy detection: a complementary AUC approach. In: IEEE Global Telecommunications Conference (GLOBECOM)
5. Atapattu S, Tellambura C, Jiang H (2011) Energy detection based cooperative spectrum sensing in cognitive radio networks. IEEE Trans Wirel Commun 10(4):1232–1241
6. Atapattu S, Tellambura C, Jiang H (2011) Spectrum sensing via energy detector in low SNR. In: Proceedings of the IEEE International Conference on Communications (ICC)
7. Atapattu S, Tellambura C, Jiang H (2014) Energy detection for spectrum sensing in cognitive radio. Springer, New York
8. Banjade VRS, Tellambura C, Jiang H (2014) Performance of p-norm detector in AWGN, fading, and diversity reception. IEEE Trans Veh Technol 63(7):3209–3222. https://doi.org/10.1109/TVT.2014.2298395
9. Banjade VRS, Tellambura C, Jiang H (2015) Approximations for performance of energy detector and p-norm detector. IEEE Commun Lett 19(10):1678–1681
10. Bharadia D, Katti S (2014) Full-duplex MIMO radios. In: Proceedings of the 11th USENIX Symposium on Networked System, Design and Implementation (NSDI'14), Seattle, pp 359–372
11. Bhargavi D, Murthy CR (2010) Performance comparison of energy, matched-filter and cyclostationarity-based spectrum sensing. In: 2010 IEEE 11th International Workshop on Signal Processing Advances in Wireless Communications (SPAWC), pp 1–5. https://doi.org/10.1109/SPAWC.2010.5670882
12. Chen Y (2010) Improved energy detector for random signals in Gaussian noise. IEEE Trans Wirel Commun 9(2):558–563
13. Deng R, Chen J, Cao X, Zhang Y, Maharjan S, Gjessing S (2013) Sensing-performance tradeoff in cognitive radio enabled smart grid. IEEE Trans Smart Grid 4(1):302–310. https://doi.org/10.1109/TSG.2012.2210058
14. Dhungana Y, Tellambura C (2012) New simple approximations for error probability and outage in fading. IEEE Commun Lett 16(11):1760–1763
15. Dhungana Y, Tellambura C (2013) Uniform approximations for wireless performance in fading channels. IEEE Trans Commun 61(11):4768–4779
16. Digham F, Alouini MS, Simon MK (2007) On the energy detection of unknown signals over fading channels. IEEE Trans Commun 55(1):21–24
17. Gavrilovska L, Denkovski D, Rakovic V, Angjelichinoski M (2014) Medium access control protocols in cognitive radio networks: overview and general classification. IEEE Commun Surveys Tutor 16(4):2092–2124
18. Goldsmith A (2005) Wireless communications. Cambridge University Press
19. Haykin S (2005) Cognitive radio: brain-empowered wireless communications. IEEE J Sel Areas Commun 23(2):201–220. https://doi.org/10.1109/JSAC.2004.839380
20. Herath S, Rajatheva N, Tellambura C (2009) On the energy detection of unknown deterministic signal over Nakagami channels with selection combining. In: Proceedings of the IEEE Canadian Conference on Electrical and Computer Engineering
21. Herath SP, Rajatheva N, Tellambura C (2011) Energy detection of unknown signals in fading and diversity reception. IEEE Trans Commun 59(9):2443–2453
22. Horgan D, Murphy CC (2010) Voting rule optimisation for double threshold energy detector-based cognitive radio networks. In: 2010 4th International Conference on Signal Processing and Communication Systems, pp 1–8. https://doi.org/10.1109/ICSPCS.2010.5709679
23. Khan AA, Rehmani MH, Rachedi A (2016) When cognitive radio meets the internet of things? In: 2016 International Wireless Communications and Mobile Computing Conference (IWCMC), pp 469–474. https://doi.org/10.1109/IWCMC.2016.7577103
24. Khan AA, Rehmani MH, Reisslein M (2016) Cognitive radio for smart grids: survey of architectures, spectrum sensing mechanisms, and networking protocols. IEEE Commun Surveys Tutor 18(1):860–898. https://doi.org/10.1109/COMST.2015.2481722

25. Kusaladharma S, Tellambura C (2012) Aggregate interference analysis for underlay cognitive radio networks. IEEE Wirel Commun Lett 1(6):641–644. https://doi.org/10.1109/WCL.2012.091312.120600
26. Kusaladharma S, Tellambura C (2013) On approximating the cognitive radio aggregate interference. IEEE Wirel Commun Lett 2(1):58–61. https://doi.org/10.1109/WCL.2012.101812.120671
27. Lee WY, Akyildiz IF (2008) Optimal spectrum sensing framework for cognitive radio networks. IEEE Trans Wirel Commun 7(10):3845–3857. https://doi.org/10.1109/T-WC.2008.070391
28. Liang YC, Zeng Y, Peh E, Hoang AT (2008) Sensing-throughput tradeoff for cognitive radio networks. IEEE Trans Wirel Commun 7(4):1326–1337
29. Masonta MT, Mzyece M, Ntlatlapa N (2013) Spectrum decision in cognitive radio networks: a survey. IEEE Commun Surveys Tutor 15(3):1088–1107
30. Medeisis A, Holland O (2014) Cognitive radio policy and regulation. Springer
31. Moghimi F, Nasri A, Schober R (2011) Adaptive L_p-norm spectrum sensing for cognitive radio networks. IEEE Trans Commun 59(7):1934–1945
32. Molisch A (2011) Wireless communications. Wiley-IEEE Press
33. Nuttall AH (1972) Some integrals involving the Q function. Naval Underwater Systems Center (NUSC), Technical report
34. Qiu RC, Chen Z, Guo N, Song Y, Zhang P, Li H, Lai L (2010) Towards a real-time cognitive radio network testbed: architecture, hardware platform, and application to smart grid. In: 2010 Fifth IEEE Workshop on Networking Technologies for Software Defined Radio Networks (SDR), pp 1–6. https://doi.org/10.1109/SDR.2010.5507920
35. Quan Z, Cui S, Sayed A, Poor H (2009) Optimal multiband joint detection for spectrum sensing in cognitive radio networks. IEEE Trans Signal Process 57(3):1128–1140
36. Riihonen T, Wichman R (2014) Energy detection in full-duplex cognitive radios under residual self-interference. In: 2014 9th International Conference on Cognitive Radio Oriented Wireless Networks and Communications (CROWNCOM), pp 57–60. https://doi.org/10.4108/icst.crowncom.2014.255395
37. Rugini L, Banelli P, Leus G (2013) Small sample size performance of the energy detector. IEEE Commun Lett 17(9):1814–1817
38. Rugini L, Banelli P, Leus G (2016) Spectrum sensing using energy detectors with performance computation capabilities. In: 2016 24th European Signal Processing Conference (EUSIPCO), pp 1608–1612
39. Shahraki HS (2015) Opportunistic usage of television white space with respect to the long term evolution-advanced parameters. IET Commun 9(9):1240–1247
40. Sharma Banjade V, Tellambura C, Jiang H (2014) Performance of p-norm detector in AWGN, fading and diversity reception. IEEE Trans Veh Technol 63(7):3209–3222
41. Sharma Banjade VR, Tellambura C, Jiang H (2015) Asymptotic performance of energy detector in fading and diversity reception. IEEE Trans Commun 63(6):2031–2043
42. Sofotasios P, Rebeiz E, Zhang L, Tsiftsis T, Cabric D, Freear S (2013) Energy detection based spectrum sensing over κ-μ and κ-μ extreme fading channels. IEEE Trans Veh Technol 62(3):1031–1040
43. Tellambura C (1996) Evaluation of the exact union bound for trellis-coded modulations over fading channels. IEEE Trans Commun 44(12):1693–1699. https://doi.org/10.1109/26.545899
44. Tellambura C, Annamalai A, Bhargava VK (2003) Closed form and infinite series solutions for the MGF of a dual-diversity selection combiner output in bivariate Nakagami fading. IEEE Trans Commun 51(4):539–542. https://doi.org/10.1109/TCOMM.2003.810870
45. Tellambura C, Mueller AJ, Bhargawa VK (1997) Analysis of M-ary phase-shift keying with diversity reception for land-mobile satellite channels. IEEE Trans Veh Technol 46(4):910–922. https://doi.org/10.1109/25.653065
46. Tervonen J, Mikhaylov K, Piesk S, Jms J, Heikkil M (2014) Cognitive internet-of-things solutions enabled by wireless sensor and actuator networks. In: 2014 5th IEEE Conference on Cognitive Infocommunications (CogInfoCom), pp 97–102. https://doi.org/10.1109/CogInfoCom.2014.7020426

47. Urkowitz H (1967) Energy detection of unknown deterministic signals. Proc IEEE 55(4): 523–531
48. Wang Q, Yue DW (2009) A general parameterization quantifying performance in energy detection. IEEE Signal Process Lett 16(8):699–702
49. Wang Z, Giannakis G (2003) A simple and general parameterization quantifying performance in fading channels. IEEE Trans Commun 51(8):1389–1398
50. Yucek T, Arslan H (2009) A survey of spectrum sensing algorithms for cognitive radio applications. IEEE Commun Surveys Tutor 11(1):116–130. https://doi.org/10.1109/SURV.2009.090109